ISSN: 0975-8585

Research Journal of Pharmaceutical, Biological and Chemical Sciences

Synthesis of Nano-crystalline Pyrite FeS_2 By Mechanical Alloying: Structural, Microstructural, Hyperfine and Optical Investigations.

Sifi GHRIEB*[1], Abdelmalik DJEKOUN[1], Abderrahim BENABBAS[2], Naouam BOUDINAR[1], Mohamed BENABDESLEM[1], and Bouguerra BOUZABATA[1].

[1]Laboratory of Magnetism and Spectroscopy of Solids, Faculty of Sciences, University of Annaba, 23000 Annaba, Algeria
[2]Laboratory of Processes for Materials, Energy, Water and Environment, Faculty of Sciences and Technology, University of Bouira, 10000 Bouira, Algeria.

ABSTRACT

Nanostructured pure FeS_2 (Pyrite) powders have been prepared from metallic iron and sulphur, using high energy planetary ball-mill. Changes in structural, morphological, hyperfine and optical properties of the powders during mechanical alloying have been examined by X-ray diffraction, scanning electron microscopy, Fe Mössbauer spectroscopy and spectrophotometry. Reducing the reaction time was challenged by optimizing milling speed and milling intervals duration. This attempt was successfully achieved down to12 h for obtaining pure pyrite phase. Its lattice parameter has been found to increase up to 5.460(3) Å after 72 hours of milling in relation with the growing creation of defects in the structure. After 24 hours milling, crystallite size saturates around 60 nm while root-mean-square strain exhibits small fluctuations around 0.07 %. The powder microstructure has the aspect of agglomeration of refined micro-flakes. The obtention of pyrite FeS_2 is also attested by the corresponding doublet in Mössbauer spectra. The energy gap value confirms the potential application for electro-optical devices.

Keywords: Mechanical alloying, Nanopowders, pyrite, X-ray diffraction, Scanning Electron Microscopy, Mössbauer spectroscopy.

Corresponding author

ISSN: 0975-8585

INTRODUCTION

Mechanical alloying is a solid-state powder processing method, firstly developed by Benjamin and his Co-workers [1-3] in 1970s, well established as important route of synthesis of varieties of materials, such as amorphous alloys, nanocrystalline materials, intermetallic compounds, composites and nanocomposites[4-14]. This process consists of repeated welding-fracturing-welding of a mixture of powder particles in a high-energy ball mill; the effects of ball milling on physical or chemical reactions are due to the local high temperature and pressure attained during the ball impacts. Consequently, the milling process will promote the diffusion of chemical species and make it possible the formation of equilibrium or non-equilibrium phases to be performed at lower temperature with respect to the conventional solid state route. Furthermore, this mechanism leads to finer particles with a narrower particle size distribution and randomly orientated interfacial boundaries.

The energy transfer depends on many factors such as the type of mill, nature of powders, speed and duration of milling, size of the balls as well as dry or wet milling. Iron sulphides are considered as advanced inorganic materials in relevant applications, such as high-energy density batteries, photo-electrolysis, solar energy conversion, precursors for the synthesis of pnictides superconductors and chalcogenides [15–19]. Pyrite FeS_2 produced by mechanical milling was investigated by several authors[20-25]. Among these works, three dealt with the mechano-synthesis of Pyrite from powder mixture of elemental Fe and S. In the study of Lin et al.[21], only the troilite phase $Fe_{1-x}S$ was obtained at the end of milling while for Chin et al.[22] and Jiang et al.[20], the Pyrite FeS_2 pure phase was achieved only after prolonged milling times of 72 and 110 hours respectively. The latter authors mentioned a milling speed of 200 rotations per minute in their experimental details.

In the current work, our objective was to reduce the time of phase formation of pure Pyrite; the envisaged alternative solution has been to enhance the milling speed, combined with optimized milling steps duration. This study has allowed us to divide the reaction time by approximately a factor of 3. We report here on the preparation of Pyrite FeS_2 powder by mechano-chemical reaction between Fe and S. The phase formations, as well as structural, microstructural, hyperfine and optical characteristics as function of milling time were monitored by X-ray Diffraction (XRD), Scanning Electron Microscopy (SEM), Fe Mössbauer Spectroscopy and spectrophotometry.

EXPERIMENTAL DETAILS

Mechanical alloying of mixture of elemental Fe (99.9%) and S (99.8%) powders in nominal composition ratio of 1:2, was carried out in a commercial Fritsch Pulverisette 7 planetary ball mill under argon atmosphere to prevent oxidation phenomena; the weight ratio of balls to powder was 20:1. After preliminary study, a rotation speed of 400 rpm was adopted; further higher energy has given no significant improvement. To avoid excessive heating during milling, the best results were obtained with 10 min pause time after every 30 min running time. After different milling times, the process was interrupted and small amounts of milled powders were taken out for analysis. X-rays powder diffraction experiments were performed at room temperature on a X'PERT PRO MPD Diffractometer of PANalytical equipped with a Cu-anode X-ray tube and a curved graphite monochromator in the secondary beam set which selects the $K\alpha_1$ and $K\alpha_2$ wavelengths. An acquisition time of 3 s was used per angular step of 0.04° over the 20° – 120° (2θ) range. The identification of the crystalline phases present in the samples was performed using X'Pert High Score software[26] supported with the ICDD-PDF2 database. The crystal lattice constants were refined using Celref3 software[27]; the peak fitting was carried out using Rietica software[28].The systematic error correction of the position of the peaks where performed within the software.

For the determination of crystalline perfection (crystallite size and microdefromation), a Rietveld methodology has been used. The methodology is well described in the software Fullprof (Profile Matching & Integrated Intensities Refinement of X-ray and/or Neutron Data (powder and/or single-crystal [29]).

Scanning electron microscope JEOL JSM-6360 equipped with energy dispersive x-ray detector was used for morphology and microstructure observations and chemical composition analysis.

In order to give more accurate description of the hyperfine properties, the nanoparticles were investigated by ^{57}Fe Mössbauer spectrometry. The Mössbauer spectroscopy measurements were performed in

transmission geometry at room temperature, using a constant acceleration signal spectrometer with a ^{57}Co source diffused into rhodium matrix. Mössbauer spectra were fitted using the Mosfit program[30]. The isomer shift values are quoted relative to that of α-Fe at 300 K.To study the optical characteristics of the prepared FeS_2, thin films were thermally grown onto glass substrates under a vacuum of 10^{-6}Torr, in a BALZERS coating unit. Tungsten boat heated by Joule effect was used to evaporate ball milled FeS_2 powder. The substrate temperature was maintained at 250 °C throughout deposition and the thickness d of the layers was about 0.5 μm determinate by quartz balance. The optical properties of the deposited layers by means of optical absorption have been investigated using a Perkin-Elmer λ9 (UV-VIS-NIR) spectrophotometer in the 300–2000 nm wavelength range at room temperature.

RESULTS AND DISCUSSION

X-ray Diffraction Analysis (XRD)

Figure.1 shows the XRD patterns of the mixture of starting materials iron and sulphur (0h) and of as-milled powders after 6h and 12h of milling, chosen as examples where significant changes took place. Before milling process (Figure.1a), one can distinguish, as expected, the characteristic peaks of body-centered cubic (bcc) iron α-Fe (JCPDS n° 06-0696) and orthorhombic sulphur (JCPDS n° 83-2283). After 6h of milling (Figure.1b), the formation of pyrite FeS_2 phase (JCPDS n° 42-1340) has already begun; at this stage, it is accompanied by a weak content of the non-stoichiometric iron sulphide $Fe_{1-x}S$ (JCPDS n° 75-2377) as an intermediate product of sulfurization and also by a fraction of metallic iron not yet engaged in this reaction. Disappearance of sulphur XRD peaks in this pattern is a consequence of its amorphization by the action of milling impacts, which was already mentioned by other authors[31-33]. After 12 hours of milling (Figure.1c), metallic iron is completely consumed and the obtention of pure pyrite phase is fulfilled. A the first stage of Pyrite formation, its lattice constant (~ 5.421(4) Å) is closely similar to the reference values[34]. Extension of milling time induces no decomposition of pyrite phase, in accordance with the work of Chin et al.[22], but causes linear increase of its crystal parameter (Figure.2). The gradual generation of defects in ionic structures[35-37] and particularly in Pyrite[24], is admitted to be responsible for the lattice expansion. The linear slope of this curve has to be related to the intra-crystallite quality of cationic and anionic vacancies; whereas the presence of inter-crystallite defects would have given a non-linear behaviour[38].

The effects of increasing strain and decreasing crystallite size act in the same sense for the observed width of diffraction peaks; nevertheless, their different variations versus θ make it possible to separate their individual contributions. These two effects have respectively a more Gaussian and Lorentzian characters in the peak shape; the peak fit according to the Voigt function will allow to extract the corresponding parameters (U, V, W) and γ. Furthermore, the instrumental contribution, termed (U_i, V_i, W_i) and γ_i, must be taken into account and determined by use of suitable standard (α-quartz); it exhibits a neglected strain broadening and a mean crystallite size of 1.59 μm.

The crystallite size D is given by the relation:

$$D = \frac{180\,\lambda}{\pi(\gamma - \gamma_{ins})} \qquad (1)$$

Owing to the quality of our patterns, only U parameter is refined and consequently, the effective root mean square strain e_{rms}(expressed in %) can be approximated by:

$$e_{rms} = \frac{100\pi\sqrt{U - U_{ins}}}{720\sqrt{2\ln 2}} \qquad (2)$$

The value ($U-U_{ins}$) is an estimate of the isotropic broadening. The parameter $(\gamma - \gamma_{ins})$ is a measure of the isotropic size effect[29]. The application of this approach for Pyrite FeS_2 in our samples is summarized in Figure.3. It can be depicted a rapid decrease of crystallite size between 0 and 24 hours and its stabilisation (saturation) around 60 nm. In Figure.3 also, a manifest increase of microstrain e_{rms} of pyrite FeS_2 is observed with a break point at 24 h hours. Beyond this processing time, the microstrain seems to fluctuate around a value of 0.07 %. These variations are typical of such processes[39-41];they are due to global cycles of antagonist phenomena: growth-pulverization and strain-relaxation of nanoparticles.

ISSN: 0975-8585

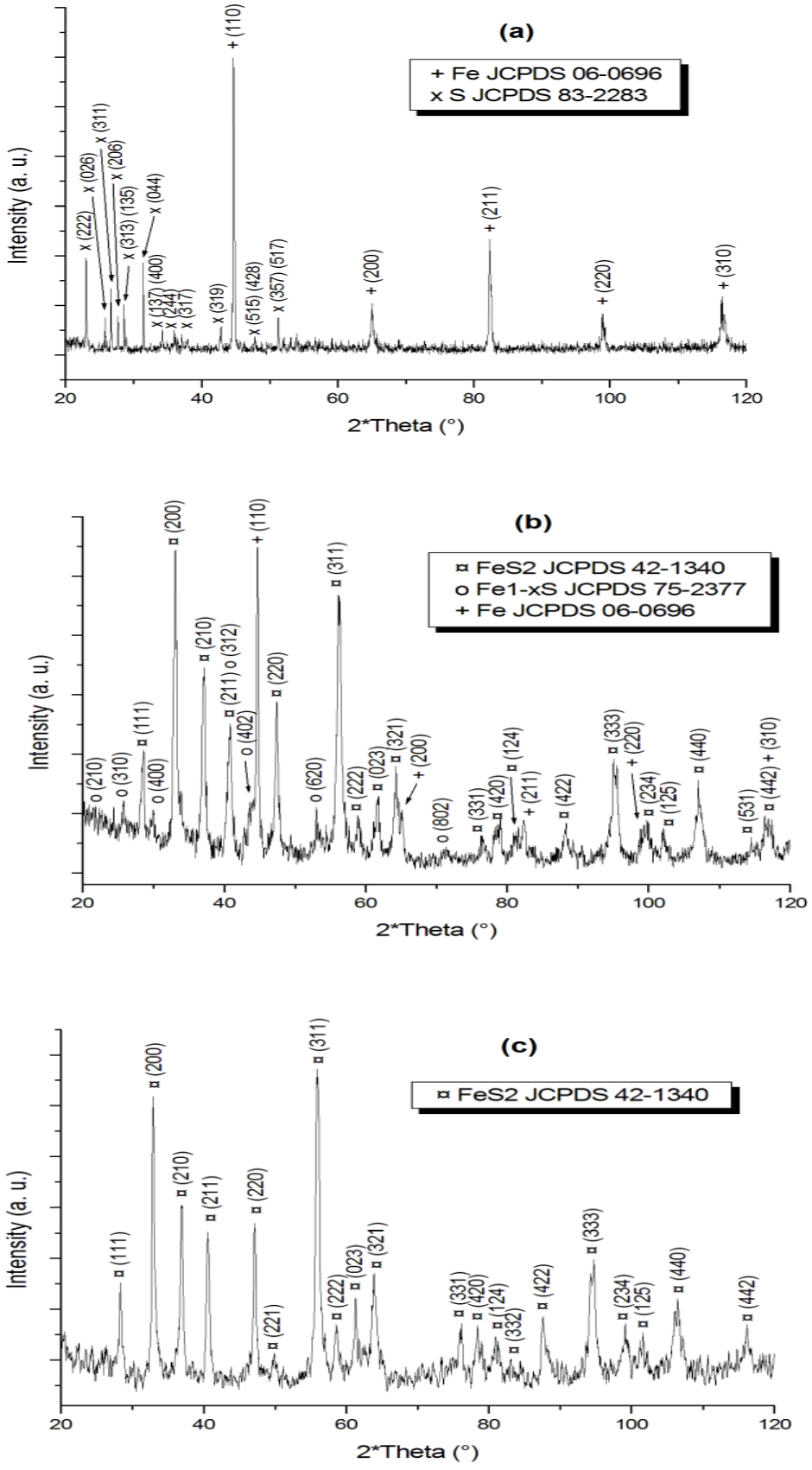

Figure 1: X-ray diffraction patterns of as-milled powders: (a) 0h, (b) after 6h, and (c) 12h.

ISSN: 0975-8585

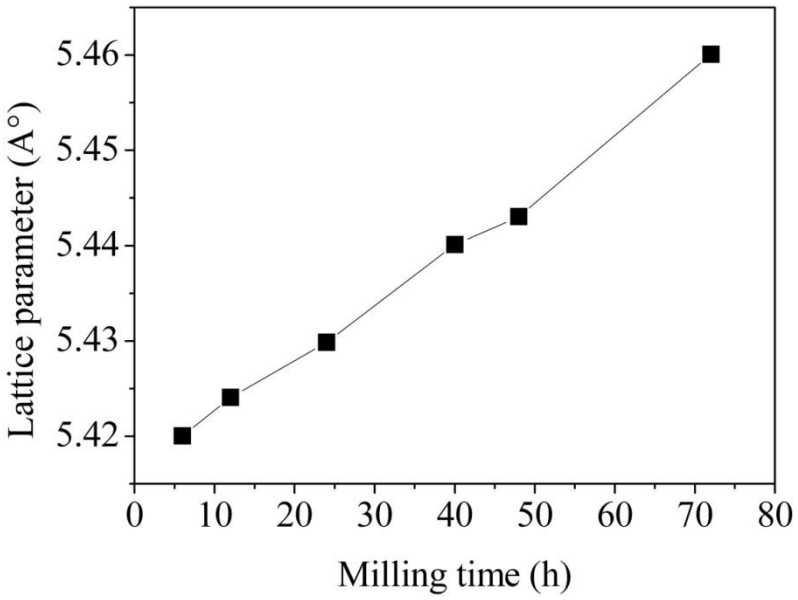

Figure 2: Evolution of the unit-cell parameter a of Pyrite FeS_2 versus time of milling.

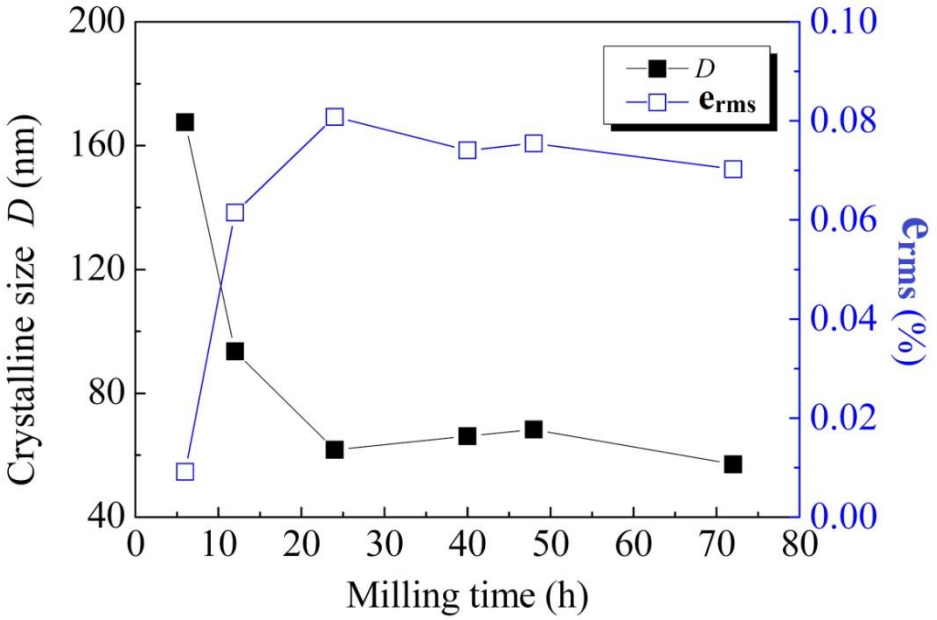

Figure 3: Evolution versus milling time of Crystallite size and microstrain of pyrite FeS_2.

Microstructural Characterization

Figure.4 illustrates the SEM micrographs of as-milled powders after various milling times. Ball milling causes a drastic change in the morphology of the powders, the particles are subjected to severe plastic deformation that introduces various crystal defects such as dislocations, vacancies, stacking faults and grain boundaries. It has been known that a critical balance between cold welding and fracturing is necessary for successful mechanical alloying, which enables powder particles to be always in contact with each other with atomically clean surfaces, thus minimizing the diffusion distance[9]. Figure.4(a) represents the morphology of the homogenised starting mixture of iron and sulphur powders before milling. One can see that the iron particles, generally of spherical shape, have a certain size distribution with approximate mean size of 2 µm;

these particles are pasted on the agglomerates of Sulphur particles having irregular morphology. This morphology constitutes a limiting step for the sulfurization reaction; the first hours of milling are consumed to destroy large sulphur agglomerates through ball impacts and iron particles as pulverizing media. As a result of intensive repeated fracturing, cold-welding, agglomeration and de-agglomeration, the powder particles are plastically deformed and, cold-welded, composite particles are formed for short milling time. With increasing milling time, the particles morphology will change into a flake or platelet shape due to compressive forces generated by ball-powder-ball collisions, which can be regarded asmicro-forging of the powder particles. For intermediate milling times, important changes occur especially in particles morphology in comparison with those in the initial stage and cold-welding process becomes prevailing. The lamellar structure is progressively refined and convoluted by repeated flattening, fracturing and welding actions. Fracture and welding during shocks are the two basic events which produce a permanent exchange of matter among powder particles. During collisions, powder particles are subjected to high stresses, which are estimated to be about of 200 MPa for steel balls in a Spex millto some GPa in a planetary mill, for laps of time of milliseconds[42-45].This is observed in the micrograph of the powder after 6 h of milling (Figure.4(b)); the agglomerated particles present irregular shapes and sizescan be associated, on the basis of XRD analysis to the mixture of FeS_2 and $Fe_{1-x}S$ phases. Some residual particles of iron and sulphur are still present. After milling time of 12 h, the microstructure of the particles appears to beglobally homogeneous (Figure.4(c)), which supports the XRD results. These SEM micrographs are typical of materials prepared by high energy ball milling. EDS analysis (Figure.5) reveals a slight sub-stoichiometry of sulphur in the pyrite phase.

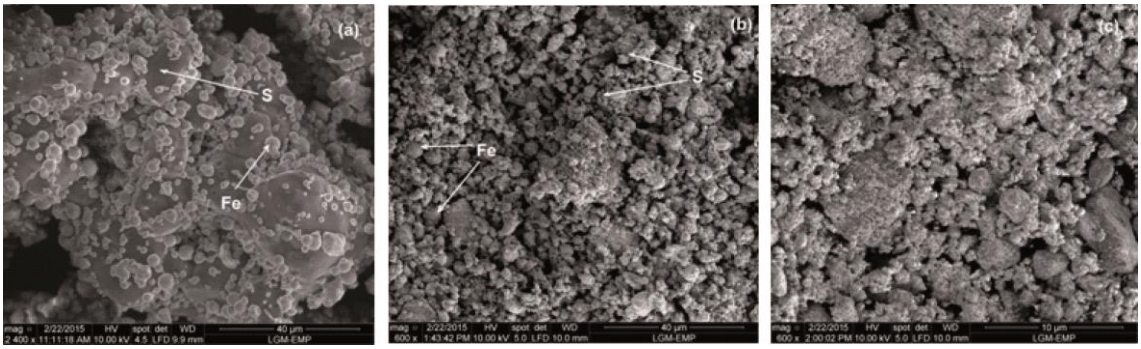

Figure 4: SEM Micrographs of powders after different milling times: (a) 0h, (b) 6h, and (c) 12h.

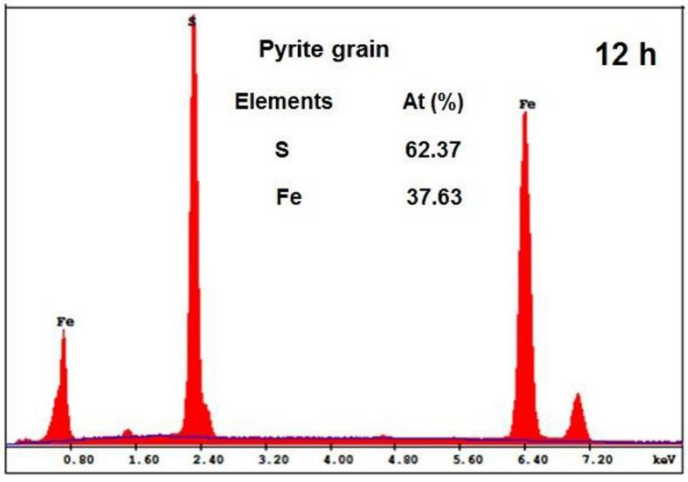

Figure 5: EDS spectra of pyrite grain in the powder after 12h of milling.

Mössbauer Analysis

Mössbauer spectra obtained at Room Temperature of the Fe-S samples, collected after different milling times,are shown in Figure.6. After 1 h of milling, the Mössbauer spectrum shows a superposition of a

paramagnetic doublet, with chemical shift = 0.32 mm/s and quadrupole splitting = 0.63 mm/s, which are expected for FeS_2 with the pyrite structure[46–49] and a magnetic sextet characterized by a hyperfine field of H = 32.96 T attributed to un-reacted iron. One can also note that the Mössbauer spectrum corresponding to 6 h of milling (Figure.6) exhibits a mixture of α-Fe magnetic sextet and two paramagnetic doublets. The first one, having a quadrupole splitting of about 0.610 mm/s and an isomer shift of 0.31 mm/sis associated to the pyrite FeS_2 phase; these parameters are in good agreement with the literature reported values of the natural pyrite mineral[50]. The secondone, having a quadrupole splitting of 2.81 mm/s, an isomer shift of 1.25 mm/s and a relative area of about 8 %, can be is attributed to the iron sulfate $FeSO_4.H_2O$ (szomolnokite);These results are in agreement with those previously reported on such materials synthesized by mechanochemical processing[20,22,51]. The formation of $FeSO_4.H_2O$ may be due to the oxidation during mechanical milling or probably during the waiting time before the Mössbauer measurements. For the sample after 12 h of milling as well as for those after 24 h and 72 h, the Mössbauer spectra illustrate clearly the paramagnetic character of the powders with the presence of only the above cited doublets. Apart from the subsequent formation of $FeSO_4.H_2O$, the Mössbauer results confirm the XRD observations regarding the pyrite phase purity in the as-milled samples.

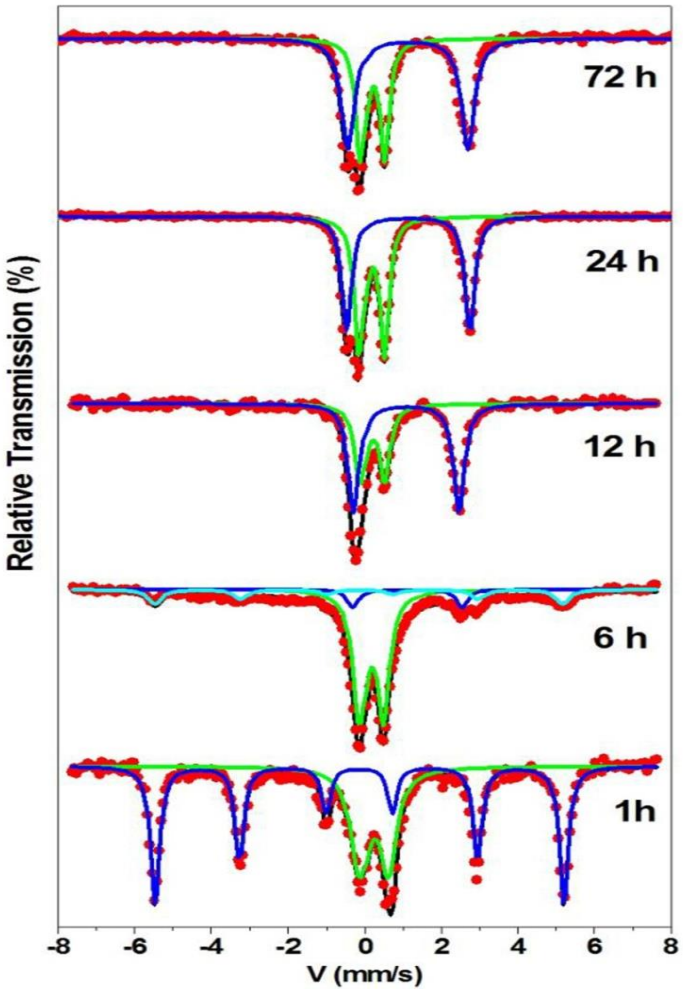

Figure 6: Mössbauer spectra of powders after different milling times.

Optical properties

Figure.7 illustrates the UV–vis-NIR absorbance spectra. As can be seen the pyrite samples exhibited a strong absorption at 450 nm. The absorption coefficient (α) of the films can be determined from the experimental transmittance data (T) using the following relation:

ISSN: 0975-8585

$$\alpha = \frac{1}{d}\ln\left(\frac{1}{T}\right) \quad (3)$$

Where d is the film thickness.

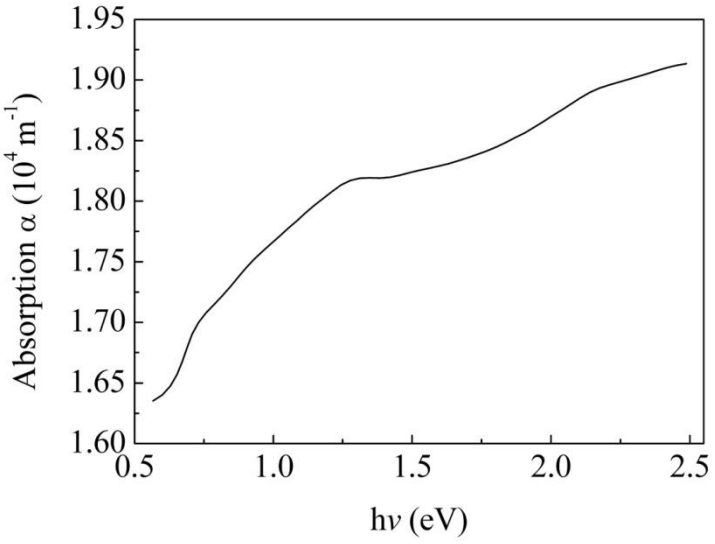

Figure 7: Absorption coefficient versus wavelength for FeS_2 thin films.

As shown in Figure.8 the value of absorption coefficient is relatively higher than 104 cm^{-1} for hν> 2.5 eV which is suitable for photovoltaic applications.

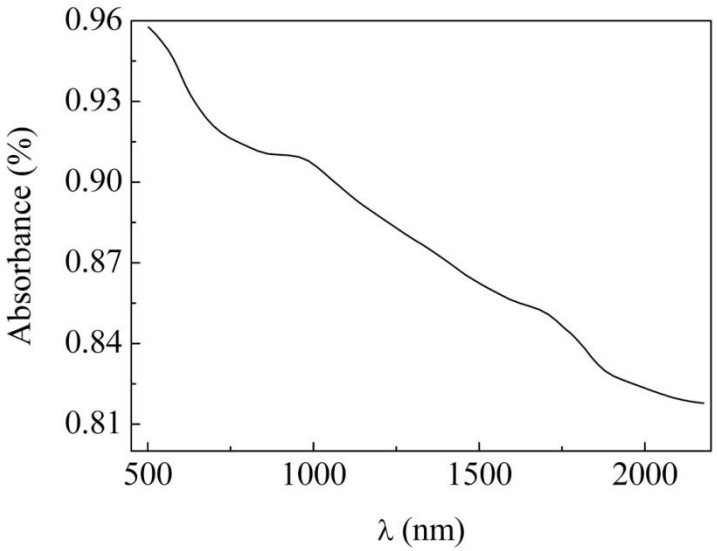

Figure 8: Variation of absorption (α) vs photon energy (hν).

As a direct band gap material, the film under study has an absorption coefficient (α) obeying the following relation for high photon energies (*hν*) and can be expressed as

$$(\alpha h\nu)^2 = A(h\nu - E_g) \quad (4)$$

Where Eg is the band gap of the FeS_2 films and A is a constant.

ISSN: 0975-8585

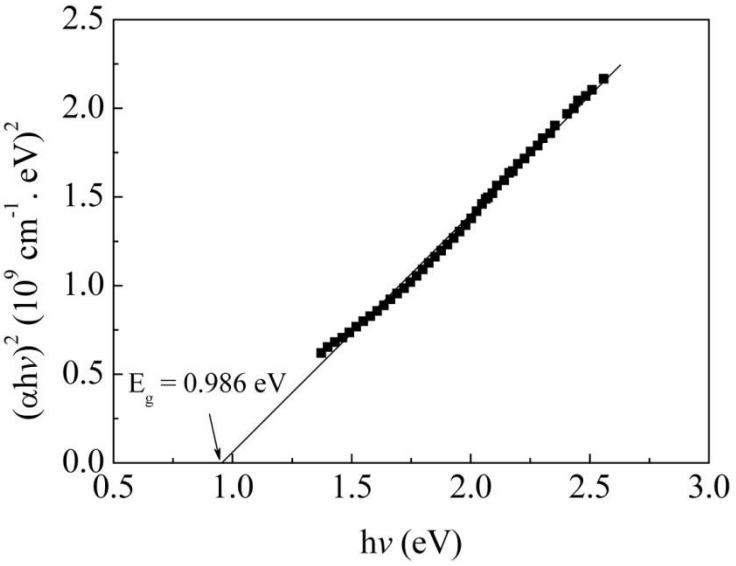

Figure 9: Plot of $(\alpha h\nu)^2$ vs photon energy hν.

The band gap energy of the samples were estimated through the Tauc relation, by plotting the tangent line of curve $(\alpha h\nu)^2$ vs hν; Eg was obtained by extrapolating the linear portion of $(\alpha h\nu)^2$ versus hν plot to $(\alpha h\nu)^2 = 0$ (see Figure.9). The energy gap (Eg) is found equal to 0.986 eV which agrees well with the reported value 0.95 eV in the literature [52,53]. This value confirms then the potential application for electro-optical devices, being synthetically prepared by ball milling. Further investigations on the optical constants of the ball milled Pyrite are ongoing by the present authors. It is well known that these constant are affected by ball milling conditions that generate new microstructure dominated by high proportion of grains boundaries and defects.

CONCLUSION

This study has confirmed the efficient influence of the rotation speed of the planetary ball mill on formation kinetic of pyrite FeS_2 nano-powders prepared by mechano-chemical processes. Indeed, a speed of 400 rpm and succession of 30 minutes intervals of milling has allowed reducing at least by a factor of 6 to only 12 hours as a maximum to obtain pure pyrite phase. This achievement was attested by XRD, SEM and Mössbauer analysis. Owing to the increase of structural defects rate, the pyrite lattice constants exhibit an expansion up to 0.7 % with prolongation of milling, whereas crystallite size and microstrain seem to saturate after 24 hours around 60 nm and 0.07 % respectively. Microstructures are characterized by agglomerated refined microflakes. In Mössbauer spectra, two types of doublets are observed; the first one is associated to the pyrite FeS_2 phase and the second one corresponding to the szomolnokite $FeSO_4.H_2O$. The energy gap value confirms the potential application for electro-optical devices, being synthetically prepared by ball milling.

ACKNOWLEDGMENTS

The authors heartily thank Dr. Hiba AZZEDDINE from University of M'Sila, Algeria, for the manuscript improvement

REFERENCES

[1] Benjamin JS. *Metal. Trans.* 1970; Vol. 1: 2943-2951.
[2] Benjamin JS, Volin TE. *Metall Trans.* 1974; Vol. 5:1929-1934.
[3] Benjamin JS, BomfordMJ. *Metal. Trans. A* 1977; Vol. 8: 1301-1305.
[4] Koch CC, Cavin OB, McKarney CG, Scarbrough JO. *Appl. Phys. Lett.* 1983; Vol. 43: 1017-1019.
[5] Schwarz RB, Koch CC. *Appl. Phys. Lett.* 1986; Vol. 49 (3): 146-148.
[6] Benjamin JS. *Metal Powder Rep.* 1990, Vol. 45:122-127.
[7] Benjamin JS. *Advances in Powder Metallurgy* 1992; Vol. 7:155-168.
[8] Koch CC. Whittenberger JD. *Intermetallics* 1996; Vol. 4: 339-355.
[9] Lü L, Lai MO: *Mechanical Alloying*, Kluwer, Academic Publishers, Massachusetts,1998,

[10] Soni PR: *Mechanical Alloying. Fundamentals and Applications*, Cambridge International Science, Cambridge, 2000
[11] Suryanarayana C. *Progress in Materials Science*2001; Vol. 46 (1-2):1-184.
[12] Djekoun A, Otmani A, Bouzabata B, Bechiri B, RandrianantoandroN, GrenecheJ.M.*Catalysis Today* 2006; Vol. 113 (3-4): 235-239.
[13] Hadef F, Otmani A, Djekoun A, Greneche JM.*J. Magnetism and Magnetic Materials* 2013; Vol. 326: 261–265.
[14] Chebli A, Djekoun A, Boudinar N, Benabdeslem M, Bouzabata B, Otmani A, Sunõl JJ.*JOM;* Vol. 68 (1): 351-361.
[15] Tributsch H. *Studies in Inorg. Chem.* 1984; Vol. 5: 277-310.
[16] Arico AS, Antonucci V, Giordano N, CreaF, Antonucci PL. *Materials Chem. and Phys.* 1991; Vol. 28 (1):75-87.
[17] Ritchie AG, Bowles P, Scattergood DP.*J. Power Sources*, 2004; Vol. 136 (2): 276-280.
[18] Shangguan E, Li F, Li J, Chang Z, LiQ, Yuan XZ, Wang H.*J. Power Sources* 2015; Vol. 291: 29-39.
[19] VivancoHK, Rodriguez EE. *J. Solid State Chem.* 2016; Vol. 242 (2): 3-21.
[20] Jiang JZ, Larsen RK, Lin R, Mørup S, Chorkendor I, Nielsen K, Hansen K, West K.*J. Solid State Chem.* 1998; Vol. 138: 114-125.
[21] Lin CK, Du CL, Chen GS, Louh RF, Lee PY, Lin HM. *Materials Science and Engineering A* 2004; Vol. 375–377: 834–838.
[22] Chin PP, Ding J, Yi JB,. Liu BH.*J. Alloys and Compounds* 2005; Vol. 390; 255–260.
[23] Akhgar BN, Pourghahramani P. *Hydrometallurgy* 2015; Vol. 153 : 83–87.
[24] Pourghahramani P,Akhgar BN. *International Journal of Mineral Processing*2015; Vol. 134: 23–28.
[25] Soori M, Zarezadeh K, SheibaniS, Rashchi F.*Advanced Powder Technology* 2016; Vol. 27: 557–63.
[26] Koninklijke Philips Electronics N.V., X'Pert High score, Philips Analytical B.V., Almelo, The Nederlands, 2001
[27] Laugier J, Bochu B. Celref version 3 (2002) Cell Parameter Refinement Program from Powder Diffraction Diagram, Laboratoire des Matériaux et du Génie Physique, Ecole Nationale Supérieure de Physique de Grenoble (INPG), France.
[28] Howard CJ, Hunter BA, Swinkels DAJ. Rietica version v4.2: *IUCR Powder Diffr.*1997, Vol. 22, pp. 21-26.
[29] http://www.ccp14.ac.uk/tutorial/fullprof/doc/fp_frame.htm
[30] Teillet J, Varret F. Unpublished Mosfit program, Université du Maine, France.
[31] Urakaev FK, Shevchenko VS,Savintsev YP. *Chemistry for Sustainable Development*2005; Vol. 13: 453–457.
[32] Nagao M, Hayashi A, Tatsumisago M. *ElectrochimicaActa*2011; Vol. 56: 6055-6059.
[33] Berbano SS, Seo I, Bischoff CM, Schuller and KE, Martin SW. *J. Non-Crystalline Solids* 2012; Vol. 358: 93–98.
[34] Brostigen G, Kjekshus A. *Acta Chem. Scand.* 1969; Vol. 23:2186-2188.
[35] Tsunekawa S, Ishikawa K, Li ZQ, Kawazoe Y,Kasuya A.*Phys. Rev. Lett.* 2000; Vol. 85:3440-3443.
[36] Li G, Goates JB, Woodfield B. *Appl Phys Lett.* 2004; Vol. 85: 2059-2061.
[37] Marinca TF, Chicinaş I, Isnard O, Pop V,Popa F.*J. Alloys and Compounds* 2011; Vol. 509: 7931-7936.
[38] Banerjee A, Gupta R, Balani K.*J. Mater. Sci.* 2015; Vol. 50: 6349-6358.
[39] Djekoun A, Bouzabata B, Otmani A,Greneche JM. *Catalysis Today* 2004; Vol. 89 (3): 319-323.
[40] Abdoli H, Ghanbari M, Baghshahi S. *Materials Science and Engineering A* 2011; Vol. 528: 6702-6707.
[41] Yadav TP, Yadav RM, Singh DP. *Nanoscience and Nanotechnology* 2012; Vol.2(3): 22-48.
[42] Schwarz RB. *Materials Science and Engineering*1988; Vol. 97: 71-78.
[43] Schwarz RB. *Materials Science Forum* 1998; Vol. 269–272: 665-674.
[44] Schaffer GB, Forester JS. *J. Mater. Sci.* 1997; Vol. 32 (12): 3157-3162.
[45] Courtney TH, Maurice D. *Scripta Mat.* 1996; Vol. 34 (1): 5-11.
[46] Garg VK, Liu YS,Puri SP. *J. Appl. Phys.* 1974; Vol. 45 (1): 70-72.
[47] Nishihara Y, Ogawa S. *J. Chem. Phys.* 1979; Vol. 71: 3796-3801.
[48] Eymery JP. *Eur. Phys. J.* 1999; Vol. 5: 115-21.
[49] Greenwood NN, Gibb TC.*Mössbauer Spectroscopy*, Chapman and Hall, London, 1971.
[50] S.P. Taneja and C.H.W. Jones:*Fuel*, 1984, Vol. 63, pp. 695-701.
[51] Paneva D, Mitova D, Manova E, Kolev H, KunevB, Mitov I.*J. of Mining and Metallurgy B* 2007; Vol. 43: 57-70.
[52] de las Herasa C, Lifante G. J. Appl. Phys.1997; 82:5132-5137.
[53] Ferrer IJ, Nevskaia DM, de lasHeras C, Sánchez C. Solid State Communications 1990; 74: 913-916